

Cold-atom double- Λ coherent population trapping clock

F.-X. Esnault,^{1,2} E. Blanshan,¹ E. N. Ivanov,³ R. E. Scholten,⁴ J. Kitching,¹ and E. A. Donley^{1,*}

¹*National Institute of Standards and Technology, Boulder, Colorado 80305, USA*

²*Centre National d'Etudes Spatiales, 18 Avenue Edouard Belin, 31400 Toulouse, France*

³*School of Physics, The University of Western Australia, Crawley, Western Australia 6009, Australia*

⁴*School of Physics, The University of Melbourne, Melbourne, Victoria 3010, Australia*

(Received 29 May 2013; published 31 October 2013)

Miniature atomic clocks based on coherent population trapping (CPT) states in thermal atoms are an important component in many field applications, particularly where satellite frequency standards are not accessible. Cold-atom CPT clocks promise improved accuracy and stability over existing commercial technologies. Here we demonstrate a cold-atom CPT clock based on ^{87}Rb using a high-contrast double- Λ configuration. Doppler frequency shifts are explained using a simple model and canceled by interrogating the atoms with counterpropagating light beams. We realize a compact cold-atom CPT clock with a fractional frequency stability of $4 \times 10^{-11} \tau^{-1/2}$, thus demonstrating the potential of these devices. We also show that the long-term stability is currently limited by the second-order Zeeman shift to 2×10^{-12} at 1000 s.

DOI: [10.1103/PhysRevA.88.042120](https://doi.org/10.1103/PhysRevA.88.042120)

PACS number(s): 06.20.F-, 37.10.De, 06.30.Ft, 42.62.Fi

Field-deployable atomic clocks and frequency standards are critical to many applications, including telecommunications and navigation. Field applications of chip-scale atomic clocks (CSACs) [1,2] based on coherent population trapping (CPT) [3–5] are growing rapidly because of their small size and low power consumption. Probing the atoms with light eliminates the need for a bulky microwave cavity and allows for dramatic size reduction of the physics package over clocks based on direct microwave interrogation. CSACs typically deliver short-term fractional frequency stability of $<1 \times 10^{-10}$, but the devices are fundamentally not accurate because of large systematic frequency shifts arising from high-pressure buffer gases and light shifts. The long-term fractional frequency stability of CSACs is limited by drift from these shifts, which is typically 3×10^{-11} /month after a six-month break-in period for commercial CSACs [6]. This level of drift makes CSACs unsuitable for many applications, for example, for use as primary reference clocks for telecommunications synchronization, which require accuracy at the 1×10^{-11} level [7].

In CSACs, a narrow transition linewidth is achieved through long light-atom interaction periods provided by a high-pressure buffer gas. Long interaction periods can also be realized by use of laser-cooled atoms. When limited by atom shot noise [8], a cold-atom clock based on 10^6 atoms with a 10 ms interrogation period and a 100 ms cycle period could achieve a short-term frequency stability of $1 \times 10^{-12}/\sqrt{\tau}$. While the elimination of the buffer gas removes pressure shifts, it reintroduces Doppler shifts since the atoms are free to move through the phase fronts of the interrogation field and are therefore not in the Lamb-Dicke regime [9].

In conventional CPT spectroscopy, atoms are interrogated with left- or right-circularly polarized light and are pumped into trap states in which they stop contributing to the CPT signal, reducing the resonance contrast [4]. Several schemes have been implemented that eliminate trap states and improve

the fringe contrast, including push-pull optical pumping [10] and double- Λ techniques such as $\text{lin} \perp \text{lin}$ [11] and $\text{lin} \parallel \text{lin}$ spectroscopy [12].

Ramsey interrogation with CPT interactions was first demonstrated with a thermal sodium beam and spatially separated interactions [13–16]. The method has also been used in alkali-metal vapor cells with time-separated CPT pulses [11,17]. Cold-atom Ramsey spectra have also been recently observed in the $\text{lin} \perp \text{lin}$ configuration [18]. Ramsey spectroscopy has advantages over continuous excitation in reducing light-shift and power-broadening effects [11,14,19].

Here we join the techniques of laser-cooled atoms and CPT to demonstrate a ^{87}Rb cold-atom CPT clock based on the $\text{lin} \parallel \text{lin}$ configuration probed with the time-separated Ramsey method. We derive a model that concisely explains the Doppler shifts in terms of the spatially varying phase of the CPT coherences and demonstrate a configuration with counterpropagating CPT beams that cancels these shifts. With the atoms probed symmetrically under $1g$ of acceleration (vertically), the Doppler shifts are consistent with zero and are less than 1×10^{-11} . Gravity-induced shifts in a horizontally probed clock would be limited by the alignment of the probe and should be on the 10^{-13} scale or smaller.

The double- Λ CPT scheme [Fig. 1(a)] uses a $\text{lin} \parallel \text{lin}$ bichromatic laser field with parallel linear polarization to excite two pairs of optical transitions sharing a common excited level. The bichromatic field simultaneously couples the atoms into two separate Λ systems of σ^+ and σ^- transitions connecting the ground-state sublevels $|F=1, m_F=\pm 1\rangle$ and $|F=2, m_F=\mp 1\rangle$ via the excited state $|F'=1, m_F=0\rangle$. The bichromatic frequency separation is tuned to the 6.835 GHz microwave ground-state hyperfine splitting. Several groups have used the $\text{lin} \parallel \text{lin}$ double- Λ CPT system to demonstrate high-contrast resonances in buffer-gas cells [20–24].

The first pulse in the Ramsey sequence, with duration $\tau_p = 400 \mu\text{s}$ and intensity below 1% of saturation, completely pumps the atoms into the dark state. After the Ramsey period T_R , the atomic state evolution is determined by the absorption of a probe pulse of duration $\tau_m = 50 \mu\text{s}$.

*edonley@boulder.nist.gov

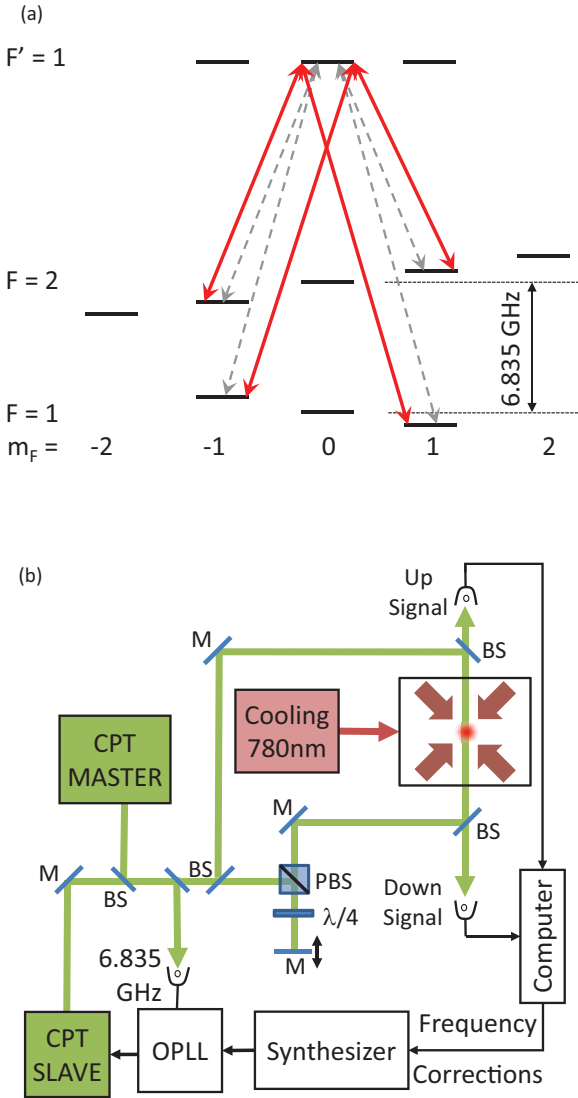


FIG. 1. (Color online) (a) Coupled energy levels of ^{87}Rb in the lin || lin CPT system (solid lines) and the transitions used to monitor the magnetic field (dashed lines). (b) Schematic of the cold-atom CPT clock. Two counterpropagating bichromatic laser fields pump and probe the cold atoms. The laser beams are vertical to maximize velocity-dependent Doppler shifts such that the shifts can be evaluated.

The two Λ systems probed in the lin || lin scheme have first-order Zeeman shifts that are equal but opposite in sign. By expanding the Breit-Rabi equation to second order, it can be shown that the Zeeman shift for the two transitions is $\Delta\nu_{\text{mag}} = 431.6 \text{ Hz/G}^2 \pm 2786 \text{ Hz/G}$ [12,25]. The opposite first-order Zeeman shifts lead to constructive interference of the Ramsey fringes for the two Λ systems only at multiples of the magnetic field that shift each Λ system by $1/2T_R$, which is 22.4 mG for $T_R = 8 \text{ ms}$ [26]. To overcome magnetic-field gradients, we use a higher field than is minimally required lift the degeneracy. We typically use a bias field of at least 90 mG, at which the second-order Zeeman shift, identical for both systems, is approximately 3.5 Hz. A field of at least 20 mG is required to separate the field-sensitive transitions from the clock transitions.

We use a differentially pumped double magneto-optical trap (MOT) system to cool and trap the atoms with separate two- and three-dimensional MOTs [27]. The volume of the vacuum system, including the pump, is $<0.2 \text{ l}$. Three pairs of Helmholtz coils cancel the residual magnetic field and establish a fixed magnetic field along the vertical direction, parallel to the CPT beams. We typically trap 10^6 atoms in a 45 ms cooling cycle and recapture 80% of the atoms from cycle to cycle after an 8 ms Ramsey period. The Ramsey period in our system is limited by magnetic-field gradients arising from the ion pump, which wash out the fringes for $T_R > 10 \text{ ms}$.

We generate the CPT light by phase-locking two commercial 795 nm laser diodes [28]. The frequency reference for the optical phase-lock loop is derived from a synthesis chain referenced to a commercial Cs atomic beam clock. The phase-lock system has a bandwidth of 8 MHz, well in excess of the laser linewidths (1 MHz), and the resulting phase error variance is 0.35 rad^2 integrated over 30 MHz. The slave laser is resonant with the $|F = 1\rangle \rightarrow |F' = 1\rangle$ transition and is also used as a repump laser. The beams are combined on a beam splitter and coupled to the experiment through a single-mode polarization-maintaining optical fiber, which ensures perfect spatial mode matching of the beams. The beams have a Gaussian profile with 3.5 mm diameter ($1/e^2$).

We use counterpropagating CPT beams to interrogate the atoms, which are produced in one of two ways. In the configuration that allows for the best Doppler-shift cancellation, the interrogation light is split into independent up and down beams and the absorption signal is measured separately for each beam [Fig. 1(b)]. In a simpler configuration, we retroreflect the interrogation light from a mirror, which degrades the cancellation of the Doppler shift because our cell is not antireflection coated and therefore the up- and down-beam intensities are not balanced. A typical Ramsey spectrum obtained by scanning the Raman detuning across the clock resonance in the retroreflected geometry is shown in Fig. 2.

For the previously studied counterpropagating CPT geometry with circularly polarized beams and room-temperature atomic vapors [29,30], true dark states where the atoms do not absorb light can be created only at positions along the z axis z_{max} , where z_{max} is defined by $2(k_1 - k_2)z_{\text{max}} = (2n + 1)\pi$. $k_i = 2\pi/\lambda_i$ are the wave numbers for the two CPT frequencies. At z_{max} , the counterpropagating CPT excitation fields interfere constructively in the atom and the atomic coherence is maximal. At other positions, there is no pure dark state and the atoms absorb some light from each beam, reaching maximum absorption at $2(k_1 - k_2)z_{\text{min}} = 2n\pi$. For the lin || lin scheme used here, the same interference of the CPT fields occurs and the amplitude of the Λ transitions is modulated as a function of position. The modulation length is the wavelength of the hyperfine ground-state splitting λ_{HF} , since $k_1 - k_2 = k_{\text{HF}} = 2\pi/\lambda_{\text{HF}}$. To optimize the signal contrast, we adjust an optical delay line in the path of the upward-propagating beam and set the initial position of the atoms to z_{max} .

When the atoms are illuminated by a CPT light field from a single direction, a Doppler shift arises from motion of the atoms along the direction of the CPT beams during the Ramsey period. The phase of the CPT interrogation field varies linearly with position, and the moving atoms are pumped into the dark state and probed in different positions. This frequency shift is

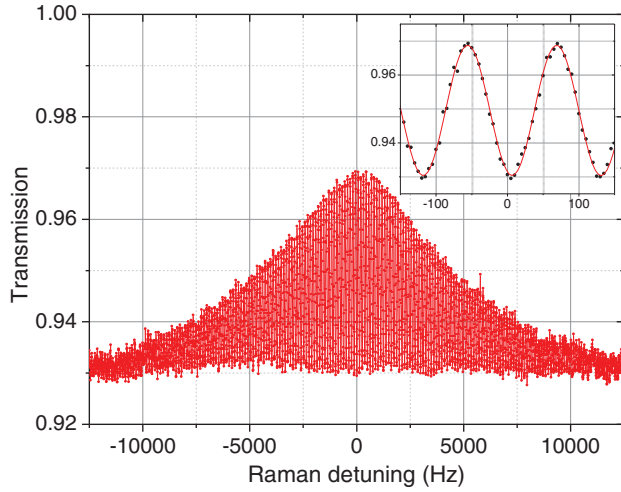


FIG. 2. (Color online) Ramsey fringes. The Λ systems are Zeeman shifted by $\pm 3/2T_R$, and the transmission is minimized near zero detuning. Each point in the spectrum was measured in 53 ms, and the signal-to-noise ratio of the spectrum is 120 in a 1 Hz bandwidth. The fringe width is 62.5 Hz, as expected for $T_R = 8$ ms. The width of the Lorentzian envelope (15 kHz) depends on the optical saturation of the pump pulse. To lock the clock, we alternately shift the phase-lock offset frequency to each side of the central fringe and steer the central offset frequency to equalize the measured absorptions. The clock stability is calculated from the frequency steering values.

given by

$$2\pi \Delta \nu_D = (k_1 - k_2)dz/T_R = k_{HF}v_{av}, \quad (1)$$

where dz is the change in position of the atom along the propagation axis during the Ramsey period and v_{av} is the average velocity. Our counterpropagating geometry excites the atoms in both directions simultaneously, which removes the spatial phase variations and introduces the spatial amplitude modulation described above. During the pump pulse, the atoms are pumped into a coherent dark state whose phase is the average phase of the upward- and downward-propagating CPT fields. During the probe pulse, the absorption in each beam is monitored independently and frequency corrections are calculated for each beam. For symmetrical excitation, the frequency shifts are equal and opposite and are $\pm(k_1 - k_2)(z_{\max} - z_m)/2\pi T_R$, where z_m is the position of the atoms during the probe pulse. Because of the symmetrical excitation during the pump pulse, the Doppler shifts depend only on the location of the atoms with respect to z_{\max} during the probe pulse.

To evaluate the shift, we dropped the atoms from initial height z_0 for a free-fall period T_f before the pump pulse. At the time of the probe pulse, the distance from z_{\max} to the atoms is

$$z_{\max} - z_m = z_0 + v_0(T_f + T_R) - \left(\frac{g}{2}\right)(T_f + T_R)^2. \quad (2)$$

The Doppler shift measured by each beam is then

$$\Delta \nu_D = \frac{\pm k_{HF}}{2\pi T_R} \left(z_0 + v_0(T_R + T_f) - \frac{g}{2}(T_f + T_R)^2 \right), \quad (3)$$

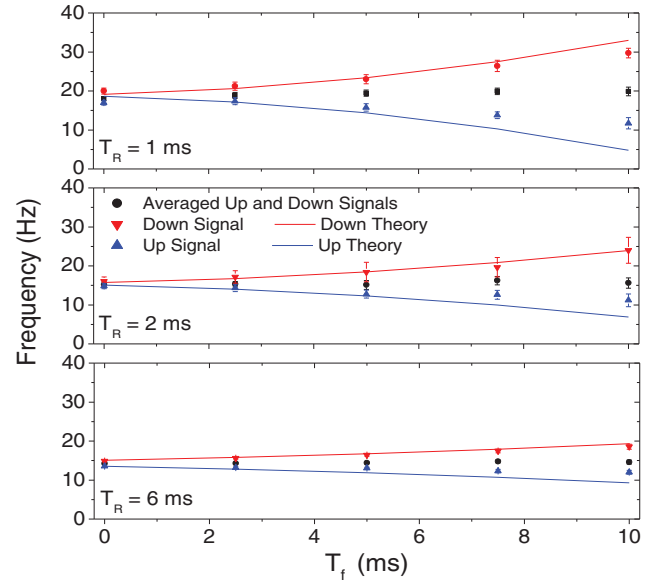


FIG. 3. (Color online) Measured frequency shifts for Ramsey periods of 1, 2, and 6 ms and varying free-fall times compared to our model from Eq. (3) with $v_0 = 0$ and $z_0 = 0$. For the different curves, the clock was locked with frequency corrections calculated from the average of the up and down signals, only the down signal, and only the up signal.

where the shift is positive for one beam and negative for the other. Locking the clock to the averaged frequency corrections from the up and down beams cancels the Doppler shift.

Figure 3 shows measurements of the frequency shift as a function of T_f , with $T_R = 1, 2,$ and 6 ms. The measured Doppler shifts for the up and down beams are usually slightly smaller than the values predicted by Eq. (3), because the up and down beams are both present during the probe pulse, which pulls the measurement towards the average phase and a new dark state. An offset is apparent at $T_f = 0$, indicating that at the time of the second Ramsey pulse, the atoms are not at z_{\max} . We investigated this offset by adding a relative phase shift between the upward- and downward-propagating beams by adjusting the optical delay line in the upward-propagating beam (Fig. 1). A change in the optical path length of dL moves z_{\max} by $dL/2$ and the associated frequency shift is

$$d\nu_D/dL = (k_1 - k_2)/4\pi T_R, \quad (4)$$

equal to 11.4 Hz/mm for $T_R = 1$ ms and 1.9 Hz/mm for $T_R = 6$ ms.

Figure 4 shows measured frequency shifts versus dL . There is some asymmetry for the up and down beams, and the slope for the up beam is significantly lower than predicted. The asymmetry is sensitive to collinear alignment and relative power of the up and down beams. When we blocked either the up or down beam during the probe pulse in a separate experiment, the average slope became significantly larger and was within 10% of the value predicted by Eq. (4). The measurements are also affected by a small traveling-wave component caused by reflections from the uncoated glass vacuum windows. We estimate from our measurements in Fig. 3 performed with $T_R = 6$ ms that the Doppler shift under

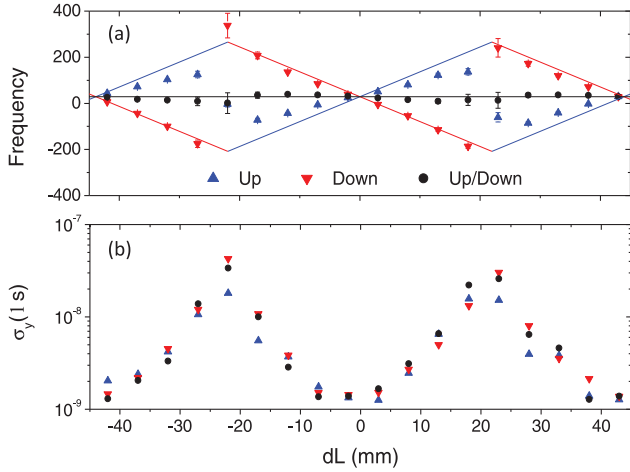


FIG. 4. (Color online) (a) Doppler frequency shift versus change in optical path length for the up beam shown with theory curves estimated from Eq. (4). Here T_R was 1 ms. (b) Measured fractional frequency stability versus dL . The positions where the clock stability deteriorates at approximately ± 22 mm correspond to values of z_{\min} .

normal clock operation cancels to $< 1 \times 10^{-11}$ residual shift for symmetric up and down interrogation. Our next-generation clock will be interrogated horizontally, and we expect the Doppler shift from gravity to be reduced to the 10^{-13} scale or lower.

The second-order Zeeman shift currently limits the long-term stability of the clock. We have quantified the Zeeman contribution to the clock drift by measuring the frequency of a field-sensitive transition (see Fig. 1) every 9 min and using the field values to calculate the time dependence of the second-order Zeeman shift. The Allan deviations for the clock frequency and the calculated Zeeman shift are shown in Fig. 5. Field drift currently limits the long-term stability at around 2×10^{-12} , corresponding to a drift in the ambient field of 0.25 mG over the 2×10^4 s measurement period. With magnetic shielding, we expect that the bias field strength can be reduced by a factor of 3, thus reducing the second-order Zeeman shift by a factor of 9 and reducing drift from stray fields by the shielding factor (100 times).

The clock frequency is also affected by the light shift (ac Stark shift), which scales with the ratio of the pump pulse length to the Ramsey period [16]. The light shift in our system includes resonant contributions from the coherent and incoherent parts of the light spectrum, as well as a small off-resonant contribution from coupling to the $F' = 2$ excited state. The resonant coherent part of the shift decreases for increasing intensity and effectively vanishes for our typical operating intensity of $20 \mu\text{W}/\text{cm}^2$. The off-resonant part of the light shift is approximately 0.1 Hz for our typical operating conditions, is proportional to intensity, and drifts at the insignificant level of 1×10^{-14} per MHz of laser detuning. For $T_R = 8$ ms, the total measured light shift is 1 Hz per MHz of detuning, and we believe that this shift arises from the incoherent part of the CPT light spectrum. Consistent with previous studies [31], the frequency lock of our master laser is stable to better than 3 kHz over long periods, and thus the

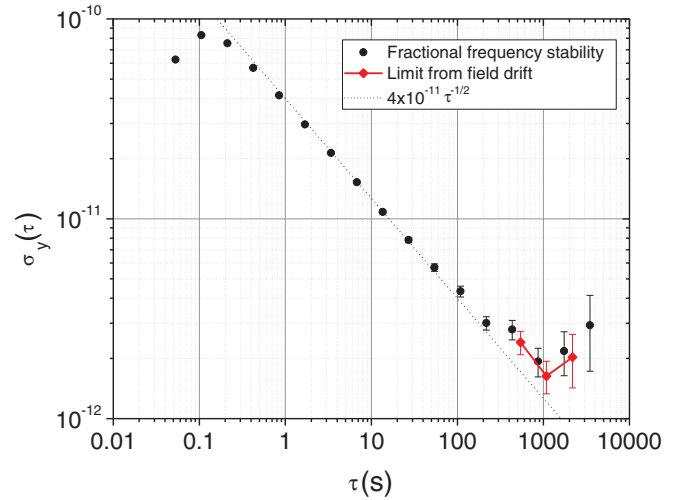


FIG. 5. (Color online) Fractional frequency stability versus integration period. The expected frequency drift from the second-order Zeeman shift as determined from *in situ* field measurements is also shown, which agrees with the observed clock drift. Here, the counterpropagating CPT beams were generated by retroreflection. The dominant noise terms that determine the short-term stability arise from laser frequency noise.

light shift is stable to a few parts in 10^{-13} . The sensitivity to detuning can potentially be reduced by operating at special values of the intensity ratio between the two CPT frequency components, which is an area of continued study. The light shift can also be reduced by improving the spectral purity of the interrogation light.

The cold-atom CPT clock presented here offers the potential for a field-deployable frequency reference that is accurate on the 10^{-13} scale and highly miniaturizable. We have modeled and characterized the clock sensitivity to motion of the atoms and demonstrated an implementation of the clock that uses counterpropagating light fields to cancel the motional dependence. We have also shown that the long-term stability of the clock is currently limited by Zeeman shifts in our unshielded system. With magnetic shielding and an improved cell design incorporating antireflection-coated windows, we expect to improve the long-term stability of the clock to the limits imposed by the Doppler and ac Stark shifts, which we estimate to be low on the 10^{-13} scale. The shielded system should also be able to operate with Ramsey periods that are easily double the typical 8 ms Ramsey period that we typically used for this work, which will reduce the light shifts by at least a factor of 2.

This work is funded by NIST and DARPA. NIST is an agency of the U.S. government, and this work is not subject to copyright. The views, opinions, and/or findings contained in this article are those of the authors and should not be interpreted as representing the official views or policies, either expressed or implied, of the Defense Advanced Research Projects Agency or the Department of Defense. (Approved for public release by DARPA Release No. 21197, distribution unlimited.)

- [1] S. Knappe, in *Comprehensive Microsystems* (Elsevier, Amsterdam, 2008), Vol. 3, Chap. 3.18, p. 571.
- [2] R. Lutwak, in *Proceedings of the IEEE International Frequency Control Symposium Jointly with the 21st European Frequency and Time Forum, Besancon, France, April 20–24, 2009* (IEEE, Piscataway, NJ, 2009), p. 573.
- [3] E. Arimondo, *Prog. Opt.* **35**, 257 (1996).
- [4] J. Vanier, *Appl. Phys. B* **81**, 421 (2005).
- [5] V. Shah and J. Kitching, *Adv. At. Mol. Opt. Phys.* **59**, 21 (2010).
- [6] R. Lutwak, in *Proceedings of the 43rd Annual Precise Time and Time Interval Meeting, Long Beach, CA, Nov. 14–17, 2011* (The Institute of Navigation, Manassas, VA, 2011), p. 207.
- [7] K. Shenoi, *Synchronization and Timing in Telecommunications* (BookSurge Publishing, Charleston, 2009).
- [8] G. Santarelli, Ph. Laurent, P. Lemonde, A. Clairon, A. G. Mann, S. Chang, A. N. Luiten, and C. Salomon, *Phys. Rev. Lett.* **82**, 4619 (1999).
- [9] R. H. Dicke, *Phys. Rev.* **89**, 472 (1953).
- [10] Y.-Y. Jau, E. Miron, A. B. Post, N. N. Kuzma, and W. Happer, *Phys. Rev. Lett.* **93**, 160802 (2004).
- [11] T. Zanon, S. Guerandel, E. de Clercq, D. Holleville, N. Dimarcq, and A. Clairon, *Phys. Rev. Lett.* **94**, 193002 (2005).
- [12] A. V. Taichenachev, V. I. Yudin, V. L. Velichansky, and S. A. Zibrov, *JETP Lett.* **82**, 398 (2005).
- [13] J. E. Thomas, P. R. Hemmer, S. Ezekiel, C. C. Leiby, Jr., R. H. Picard, and C. R. Willis, *Phys. Rev. Lett.* **48**, 867 (1982).
- [14] P. R. Hemmer, S. Ezekiel, and C. C. Leiby, Jr., *Opt. Lett.* **8**, 440 (1983).
- [15] P. R. Hemmer, G. P. Ontai, and S. Ezekiel, *J. Opt. Soc. Am. B* **3**, 219 (1986).
- [16] P. R. Hemmer, M. S. Shahriar, V. D. Natoli, and S. Ezekiel, *J. Opt. Soc. Am. B* **6**, 1519 (1989).
- [17] G. Pati, K. Salit, R. Tripathi, and M. Shahriar, *Opt. Commun.* **281**, 4676 (2008).
- [18] X. Chen, G. Q. Yang, J. Wang, and M. S. Zhan, *Chin. Phys. Lett.* **27**, 113201 (2010).
- [19] N. Castagna, R. Boudot, S. Guerandel, E. Clercq, N. Dimarcq, and A. Clairon, *IEEE Trans. Ultrason. Ferroelectr. Freq. Control* **56**, 246 (2009).
- [20] E. Breschi *et al.*, in *Proceedings of the IEEE International Frequency Control Symposium Jointly with the 21st European Frequency and Time Forum, Geneva, Switzerland, May 29–June 1, 2007* (IEEE, Piscataway, NJ, 2007), p. 617.
- [21] E. Breschi, G. Kazakov, R. Lammegger, G. Miletì, B. Matisov, and L. Windholz, *Phys. Rev. A* **79**, 063837 (2009).
- [22] S. A. Zibrov, I. Novikova, D. F. Phillips, R. L. Walsworth, A. S. Zibrov, V. L. Velichansky, A. V. Taichenachev, and V. I. Yudin, *Phys. Rev. A* **81**, 013833 (2010).
- [23] E. E. Mikhailov, T. Horrom, N. Belcher, and I. Novikova, *J. Opt. Soc. Am. B* **27**, 417 (2010).
- [24] K. Watabe, T. Ikegami, A. Takamizawa, S. Yanagimachi, S. Ohshima, and S. Knappe, *Appl. Opt.* **48**, 1098 (2009).
- [25] S. A. Zibrov, V. L. Velichansky, A. S. Zibrov, A. V. Taichenachev, and V. I. Yudin, *JETP Lett.* **82**, 477 (2005).
- [26] E. A. Donley, F.-X. Esnault, E. Blanshan, and J. Kitching, in *Proceedings of the 44th Annual Precise Time and Time Interval Meeting, Reston, VA, Nov. 26–29, 2012* (The Institute of Navigation, Manassas, VA, 2012), p. 327.
- [27] E. A. Salim, J. DeNatale, D. M. Farkas, K. M. Hudek, S. E. McBride, J. Michalchuk, R. Mihailovich, and D. Z. Anderson, *Quantum Inf. Process.* **10**, 975 (2011).
- [28] E. N. Ivanov, F.-X. Esnault, and E. A. Donley, *Rev. Sci. Instrum.* **82**, 083110 (2011).
- [29] C. Affolderbach, S. Knappe, R. Wynands, A. V. Tavichenachev, and V. I. Yudin, *Phys. Rev. A* **65**, 043810 (2002).
- [30] S. V. Kargapoltsev, J. Kitching, L. Hollberg, A. V. Tavichenachev, V. L. Velichansky, and V. I. Yudin, *Laser Phys. Lett.* **1**, 495 (2004).
- [31] J. Ye, S. Schwartz, P. Jungner, and J. L. Hall, *Opt. Lett.* **21**, 1280 (1996).